DE GRUYTER OPEN

*Int. J. of Applied Mechanics and Engineering, 2017, vol.22, No.4, pp.867-881*
DOI: 10.1515/ijame-2017-0056

# LOW FREQUENCY SLOSHING ANALYSIS OF CYLINDRICAL CONTAINERS WITH FLAT AND CONICAL BAFFLES

[1]V. GNITKO, [1]Y. NAUMEMKO and [1,2] E. STRELNIKOVA*
[1]Department of General Research in Power Engineering
A.N. Podgorny Institute for Mechanical Engineering Problems
2/10 Pozharsky St., Kharkiv, 61046, UKRAINE

[2]Department of Physics and Energy
V.N. Karazin Kharkiv National University
Svobody sq., 4, Kharkiv, 61022, UKRAINE
E-mails: basil@ipmach.kharkov.ua; estrel@ipmach.kharkov.ua; elena15@gmx.com

This paper presents an analysis of low-frequency liquid vibrations in rigid partially filled containers with baffles. The liquid is supposed to be an ideal and incompressible one and its flow is irrotational. A compound shell of revolution is considered as the container model. For evaluating the velocity potential the system of singular boundary integral equations has been obtained. The single-domain and multi-domain reduced boundary element methods have been used for its numerical solution. The numerical simulation is performed to validate the proposed method and to estimate the sloshing frequencies and modes of fluid-filled cylindrical shells with baffles in the forms of circular plates and truncated cones. Both axisymmetric and non-axisymmetric modes of liquid vibrations in baffled and un-baffled tanks have been considered. The proposed method makes it possible to determine a suitable place with a proper height for installing baffles in tanks by using the numerical experiment.

**Key words:** baffles, liquid sloshing, free vibrations, boundary element method, single and multi-domain approach, singular integral equations.

## 1. Introduction

The motion of liquids in partially filled tanks and containers has been the subject of many studies in the past few decades because of its frequent applications in different engineering areas such as aerospace and chemical industry, wind power engineering, transport, etc. Usually, liquid storage tanks contain oil or other flammable or toxic liquids. Destruction of these tanks by seismic or shock waves from a nearby explosion can lead to an environmental disaster.

Slosh control of propellant is a significant challenge to spacecraft stability. Mission failure has been attributed to slosh-induced instabilities in several cases as it was described by [1-2].

As the propellant level decreases throughout a mission, the effects of sloshing forces on the remaining fuel become more prominent. When the fuel tank is full or nearly so, the fuel lacks the open space to slosh. But in the latter stages of the mission, when most of the fuel has been consumed, the fuel has sufficient volume to slosh and possibly disturb the flight trajectory.

In order to restrain the fluid sloshing a common technique is to place additional sub-structures called baffles or separators within the tank as it was reported by Strandberg [3]. Baffles with orifices can be found in some contemporary road tankers carrying fuel, oils or liquefied natural gas. This kind of baffle can attenuate the impact forces on the baffle.

Baffles are commonly used as the effective means of suppressing the magnitudes of fluid slosh,

* To whom correspondence should be addressed

although only a few studies have assessed roles of baffle design factors [4-5]. Anti-slosh properties of baffle designs have been investigated through laboratory and numerical experiments employing small size tanks of different geometry [4-9]. The experimental investigation of sloshing processes is difficult and sometimes impossible for various reasons. So the basic approach for these problems is mathematical modelling with numerical methods [10-14]. The effect of size and location of baffle on sloshing frequencies has been reported only in several studies involving rectangular and a generic cross-section tank [4, 9, 11]. Jin Yan *et al*. [15] analyzed effectiveness of different baffle designs in limiting the manoeuvre-induced transient sloshing in a partly-filled tank. Theoretical and experimental research was accomplished in [16, 17] devoted to sloshing problems in rectangular, cylindrical and conical liquid tanks with baffles. The horizontal ring and vertical blade baffles and their damping effects were investigated by Liu and Lin [18]. After comparing the tanks without baffles with ones with baffles, it was found by Kashani *et al*. [19] that the sloshing mode, basic frequencies and free surface shape are all affected by baffles.

In this paper we developed the multi-domain boundary element method for solving the problems of liquid free vibrations in rigid tanks with different kinds of baffles. The benchmark tests are considered to validate the obtained results. The results of this paper allow us to extend the applicability of the boundary element method.

## 2. Mathematical formulation

### 2.1. Problem statement

The partially fluid-filled shell of revolution of an arbitrary meridian with internal baffles installed to damp sloshing is considered. The shell structure and its sketch are shown in Fig.1. The shell surface is denoted through $\sigma$ and the free surface of a liquid is $S_0$. So $\sigma = S_{\text{bot}} \cup S_w \cup S_{\text{baf}}$, where $S_w$ is the wall surface, $S_{\text{baf}} = \bigcup S^i_{\text{baf}}$ is the surface of baffles and $S_{\text{bot}}$ is the bottom surface.

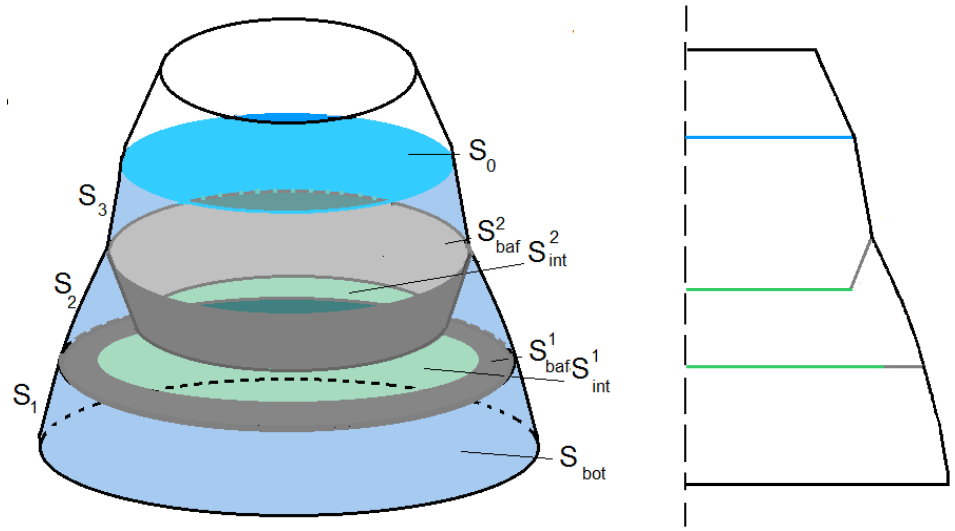


Fig.1. Shell structure with internal baffles (a) and its sketch (b).

The sloshing problems have to be described using the Navier-Stokes equations with the non-penetration condition on the walls, kinematics and dynamic boundary conditions on the free surface, but there is no general analytical or numerical solution for these equations. So it is necessary to make some simplifying assumptions.

To model the fluid domain a mathematical model has been developed that is based on the following

hypothesis: the liquid is incompressible and inviscid one; the motion of the liquid is irrotational; only small vibrations need to be considered (linear theory). Then a scalar velocity potential $\Phi(x,y,z,t)$ whose gradient represents the fluid velocity can be introduced.

Based on the existence of the velocity potential and using the Navier-Stokes equations for inviscid and irrotational flow, the governing Laplace equation can be given as

$$\Delta\Phi = \frac{\partial^2\Phi}{\partial x^2} + \frac{\partial^2\Phi}{\partial y^2} + \frac{\partial^2\Phi}{\partial z^2} = 0\,. \tag{2.1}$$

The non-penetration condition on the wetted tank surfaces (walls, bottom and baffle) is given by

$$\left.\frac{\partial\Phi}{\partial \boldsymbol{n}}\right|_{\sigma} = 0 \tag{2.2}$$

where $\boldsymbol{n}$ is an external unit normal to the wetted surface.

Introduce the function $\zeta = \zeta(x,y,t)$ that describes the form and location of the free surface.

The kinematics boundary condition assumes that a fluid particle of the free surface will always stay on that surface. It is as follows

$$\left.\frac{\partial\Phi}{\partial \boldsymbol{n}}\right|_{S_0} = \frac{\partial\zeta}{\partial t} + \frac{\partial\zeta}{\partial x}\frac{\partial\Phi}{\partial x} + \frac{\partial\zeta}{\partial y}\frac{\partial\Phi}{\partial y}\,.$$

It is assumed here that an axis *Oz* is perpendicular to the free surface, and so the function $\zeta$ is the elevation of this surface in *z* direction. With the assumption of a small elevation, the above equation can be linearized about the static free surface as follows

$$\left.\frac{\partial\Phi}{\partial \boldsymbol{n}}\right|_{S_0} = \frac{\partial\zeta}{\partial t}\,. \tag{2.3}$$

The dynamic boundary condition consists in equality of the liquid pressure on the free surface to the atmospheric one

$$\left.\frac{\partial\Phi}{\partial t} + g\zeta + a_s(t)x\right|_{S_0} = 0\,. \tag{2.4}$$

Here, $a_s(t)$ is the horizontal acceleration due to the action of seismic or shock waves, and *g* is the acceleration of gravity.

To determine the potential $\Phi$ as a solution of the boundary value problem (2.1) - (2.4) we at first solve the problem of free liquid vibrations in the rigid tank. It leads to the following representation of the velocity potential

$$\Phi = \sum_{k=1}^{M} \dot{d}_k \phi_k \tag{2.5}$$

where functions $\varphi_k$ are natural modes of liquid sloshing in the rigid tank, $d_k = d_k(t), k = \overline{1,M}$ are unknown coefficients.

To obtain modes $\varphi_k$ it is necessary to solve the next sequence of boundary value problems for auxiliary functions $\psi_k(t,x,y,z)$

$$\Delta\psi_k = 0; \quad \left.\frac{\partial\psi_k}{\partial \boldsymbol{n}}\right|_{\sigma} = 0; \quad \left.\frac{\partial\psi_k}{\partial n}\right|_{S_0} = \frac{\partial\varsigma}{\partial t}; \quad \left.\frac{\partial\psi_k}{\partial t} + g\zeta\right|_{S_0} = 0. \tag{2.6}$$

Differentiating the fourth equation in (2.6) with respect to $t$ leads to

$$\left.\frac{\partial^2\psi_k}{\partial t^2} + g\frac{\partial\zeta}{\partial t}\right|_{S_0} = 0; \qquad \left.\frac{\partial^2\psi_k}{\partial t^2} + g\frac{\partial\psi_k}{\partial \boldsymbol{n}}\right|_{S_0} = 0.$$

Look for the solution of the boundary value problem (2.6) in the next form

$$\psi_k(t,x,y,z) = e^{i\chi_k t}\phi_k(x,y,z).$$

Then the following sequence of eigenvalue problems for each $\varphi_k$ is obtained

$$\Delta\phi_k = 0; \qquad \left.\frac{\partial\phi_k}{\partial \boldsymbol{n}}\right|_{\sigma} = 0; \qquad \frac{\partial\phi_k}{\partial \boldsymbol{n}} = \frac{\chi_k^2}{g}\phi_k. \tag{2.7}$$

It follows from Eqs (2.3) and (2.5) that function $\zeta$ can be written as

$$\zeta = \sum_{k=1}^{M} d_k(t)\frac{\partial\phi_k}{\partial \boldsymbol{n}}. \tag{2.8}$$

So, the potential $\Phi$ satisfies the Laplace equation and the non-penetration boundary condition

$$\Delta\Phi = 0; \qquad \left.\frac{\partial\Phi}{\partial \boldsymbol{n}}\right|_{\sigma} = 0,$$

due to validity of relations (2.5), (2.7). It should be noted that $\Phi$ also satisfies the kinematics condition

$$\left.\frac{\partial\Phi}{\partial \boldsymbol{n}}\right|_{S_0} = \frac{\partial\zeta}{\partial t},$$

due to validity of relations (2.5), (2.8). Once functions $\varphi_k$ are defined, it is necessary to substitute them in Eqs (2.5), (2.8) and then into Eq.(2.4) and obtain finally the system of ordinary differential equations as it was done by Degtyarev *et al*. [17].

The main objective of the present study is to develop the efficient boundary element model for determining the natural sloshing frequencies of axisymmetric and non-axisymmetric modes of liquid vibrations in rigid baffled tanks.

In a case of harmonic vibrations we have to represent the unknown functions $d_k = d_k(t)$ in the form

$$d_k(t) = D_k \exp(i\omega t)$$

where ω is the liquid vibration frequency, $D_k$ are unknown constants. It leads to the following expression

$$\sum_{k=1}^{M} \ddot{d}_k \phi_k + \sum_{k=1}^{M} d_k \chi_k^2 \phi_k = 0,$$

and then one can conclude that $\omega = \chi_1, \chi_2, ...\chi_M$ are natural frequencies.

### 2.2 Multi-domain boundary element model for axisymmetric geometry

To define functions $\varphi_k$ we use the boundary element method in its direct formulation proposed by *C.* Brebbia [20]. Dropping indexes *k* we can write the main relation in the form

$$C(P_0)\phi(P_0) = \iint_S q \frac{1}{|P - P_0|} dS - \iint_S \phi \frac{\partial}{\partial n} \frac{1}{|P - P_0|} dS \tag{2.9}$$

where $S = \sigma \cup S_0$, and $C(P_0)$ depend on the internal spatial angle at the source point $P_0$; the function φ, defined on the surface σ, presents the pressure on the moistened shell surface and the function $q = \dfrac{\partial \phi}{\partial \boldsymbol{n}}$, defined on the free surface $S_0$, is the flux.

To apply the multi-domain approach we divide the fluid domain into *K* sub-domains $\Omega_k$ $(k = 1,2,...K)$ shown in Fig.2. Here we introduce the artificial interface surfaces denoted as $S_{\text{int}}^k (k = 1,2,...K-1)$. The shell wall surfaces in *k*-th domain are denoted as $S_k (k = 1,2,...,K)$, $S_{\text{bot}}$ denotes the bottom surface and $S_{\text{baf}}^k (k = 1,2,...,K-1)$ are the surfaces of baffles.

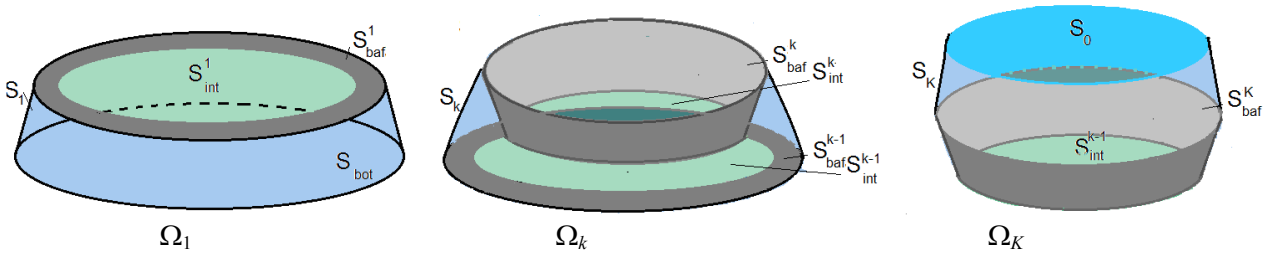


Fig.2. Fluid sub-domains: $\Omega_1$, $\Omega_k$, …$\Omega_K$.

The main idea of using the boundary element method for the fluid calculation domain divided by two or multiple sub-domains consists in the following. The influence of each domain on the neighboring one is taken into account by introducing the influence matrix. This matrix correlates the velocity potential values on the interface surface to their fluxes.

This allows us to obtain the final system of integral equations in terms of only free surface nodal quantities. After discretizating the fluid boundary into boundary elements we obtain a system of linear algebraic equations relative to unknown potential values supposing the fluxes are given.

In the considered case of free vibrations we obtain the general algebraic eigenvalue problem [17, 21]. The following denotations are used there

$$\sigma_1 = S_1 \cup S_{\text{bot}} \cup S_{\text{baf}}^1, \quad \sigma_k = S_k \cup S_{\text{baf}}^{k-1} \cup S_{\text{baf}}^k, \quad k = 2,...,K-1, \quad \sigma_K = S_K \cup S_{\text{baf}}^{K-1},$$

for wetted rigid surfaces of the structure. The boundaries of fluid sub-domains $\Omega_k\left(k = 1,2,...K\right)$ are denoted as

$$\Sigma_1 = \sigma_1 \cup S_{\text{int}}^1, \ldots . \Sigma_k = \sigma_k \cup S_{\text{int}}^{k\text{-}1} \cup S_{\text{int}}^k \left(k = 2,...,K-1\right),$$

and $$\Sigma_K = \sigma_K \cup S_{\text{int}}^{K\text{-}1}.$$

The following denotations for the arrays of potential's values in nodes at the rigid boundaries of the tank in sub-domains $\Omega_k$ are used

$$\phi^k = \phi\left(x,y,z\right)\big|_{\sigma_k}, \qquad k = 1, 2,...,K.$$

The fluxes on the rigid surfaces are equal to zero due to the non-penetration condition.

The arrays of potential and flux values in nodes of the interface surfaces $S_{\text{int}}^k$ are denoted as

$$\phi_{\text{int}}^{k1} = \phi\left(x,y,z\right)\big|_{S_{\text{int}}^k}; \qquad q^{k1} = q\left(x,y,z\right)\big|_{S_{\text{int}}^k}, \qquad \text{if} \qquad S_{\text{int}}^k \subset \Sigma_k;$$

$$\phi_{\text{int}}^{k2} = \phi\left(x,y,z\right)\big|_{S_{\text{int}}^k}, \ q^{k1} = q\left(x,y,z\right)\big|_{S_{\text{int}}^k}; \ \text{if} \ \ S_{\text{int}}^k \subset \Sigma_{k+1}; \ \ P = \left(r,z,\theta\right); \ \ \left(k = 1,2,...,K-1\right),$$

respectively. On the free surface $S_0$ the arrays of potential and flux values in nodes are denoted as $\varphi_0$ and $q_0 = \dfrac{\partial\phi}{\partial \boldsymbol{n}}\Big|_{S_0}$, respectively.

On the interface surfaces $S_{\text{int}}^k$ the next equalities are valid [20]

$$\phi_{\text{int}}^{k1} = \phi_{\text{int}}^{k2}; \qquad q^{k1} = -q^{k2}.$$

So there are only two sets of unknowns on these surfaces

$$\phi_{\text{int}}^{k1} = \phi_{\text{int}}^{k2} = \phi_{\text{int}}^{k}; \qquad q^{k1} = q^{k}; \quad q^{k2} = -q^{k}.$$

It should be noted that there are two types of kernels in the integral operators introduced above. Namely, we have

$$A\left(S,\sigma\right)\psi = \iint\limits_S \psi \frac{\partial}{\partial \boldsymbol{n}} \frac{1}{\left|P - P_0\right|} dS; \quad B\left(S,\sigma\right)\psi = \iint\limits_S \psi \frac{1}{\left|P - P_0\right|} dS; \quad P_0 \in \sigma. \tag{2.10}$$

Introducing the next denotations $\tilde{S}_{2k+1} = \sigma_k$, $(k = 0,1,...,K-1)$; $\tilde{S}_{2k} = S_{\text{int}}^k$ $(k = 1,2,...,K-1)$ and $\tilde{S}_{2K} = S_0$ one can obtain the following expressions

$$A_{ij} = \delta_{ij} C(P_0) + A(\tilde{S}_i, \tilde{S}_j); \quad B_{ij} = B(\tilde{S}_i, \tilde{S}_j), \qquad i, j = 1,2,...,2K.$$

o the system of integral equations for the first fluid domain $\Omega_1$ may be written in the following form

$$\begin{aligned} &A_{11}\phi^1 + A_{12}\phi_{\text{int}}^1 = B_{12}q^1; \quad P_0 \in \sigma_1; \\ &A_{21}\phi^1 + A_{22}\phi_{\text{int}}^1 = B_{22}q^1; \quad P_0 \in S_{\text{int}}^1. \end{aligned} \tag{2.11}$$

From Eqs (2.11) one can obtain the expressions for $\varphi^1$ and $\phi_{\text{int}}^1$ as it was done in [8, 17]

$$\phi^1 = F_1 q^1; \qquad \phi_{\text{int}}^1 = F_{1i} q^1.$$

Here

$$F_1 = A_\phi^{-1} B_{q1}; \quad A_\phi = A_{11} - \frac{1}{2\pi} A_{12} A_{21}; \quad B_{q1} = B_{12} - \frac{1}{2\pi} A_{12} B_{22;}; \quad F_{1i} = \frac{1}{2\pi}(B_{22} - A_{21} F_1).$$

Thus, the equation that correlates the flow flux $q^1$ of the interface surface $S_{\text{int}}^1$ to its velocity potential $\phi_{\text{int}}^1$ is obtained, namely

$$\phi_{\text{int}}^1 = F_{1i} q^1 \tag{2.12}$$

where $F_{1i}$ is the influence matrix.

According to [19] the system of integral equations for the second fluid domain $\Omega_2$ may be written as

$$\begin{aligned} &A_{22}\phi_{\text{int}}^1 + A_{23}\phi^2 + A_{24}\phi_{\text{int}}^2 + B_{22}q^1 = B_{24}q^2; \quad P_0 \in S_{\text{int}}^1 = \tilde{S}_2; \\ &A_{32}\phi_{\text{int}}^1 + A_{33}\phi^2 + A_{34}\phi_{\text{int}}^2 + B_{32}q^1 = B_{34}q^2; \quad P_0 \in \sigma_2 = \tilde{S}_3; \\ &A_{42}\phi_{\text{int}}^1 + A_{43}\phi^2 + A_{44}\phi_{\text{int}}^2 + B_{42}q^1 = B_{44}q^2; \quad P_0 \in S_{\text{int}}^2 = \tilde{S}_4. \end{aligned} \tag{2.13}$$

With Eqs (2.12), (2.13) and according to [19] it is possible to express $\phi_{\text{int}}^2 = F_{2i} q^2$ along the interface surface $S_{\text{int}}^2 = \tilde{S}_4$.

Equations similar to (2.13) can be written for each fluid sub-domain $\Omega_k (k = 2,...,K-1)$ as follows

$$A_{2k,2k}\phi_{\text{int}}^{k-1} + A_{2k,2k+1}\phi^{k} + A_{2k,2k+2}\phi_{\text{int}}^{k} + B_{2k,2k}q^{k-1} = B_{2k,2k+2}q^{k};\quad P_0 \in \tilde{S}_{2k};$$

$$A_{2k+1,2k}\phi_{\text{int}}^{k-1} + A_{2k+1,2k+1}\phi^{k} + A_{2k+1,2k+2}\phi_{\text{int}}^{k} + B_{2k+1,2k}q^{k-1} = B_{2k+1,2k+2}q^{k};\quad P_0 \in \tilde{S}_{2k+1}; \qquad (2.14)$$

$$A_{2k+2,2k}\phi_{\text{int}}^{k-1} + A_{2k+2,2k+1}\phi^{k} + A_{2k+2,2k+2}\phi_{\text{int}}^{k} + B_{2k+2,2k}q^{k-1} = B_{2k+2,2k+2}q^{k};\quad P_0 \in \tilde{S}_{2k+2}.$$

From Eqs (2.14) and the relation

$$\phi_{\text{int}}^{k-1} = F_{k-1,i}q^{k-1},$$

one can obtain that $\phi_{\text{int}}^{k} = F_{k,i}q^{k}$ on the interface surface $S_{\text{int}}^{k} = \tilde{S}_{2k}$, and for $k = K$ it will be $\phi_{\text{int}}^{K} = \phi_0 = F_{K,i}q^{K}\big|_{S_{2K}}$.

But $\tilde{S}_{2K} = S_0$ and so we have $q^{K} = q_0 = \omega^2\phi_0$.

Hence

$$\phi_0 = \omega^2 F_{K,i}\phi_0, \qquad (2.15)$$

at the free surface. So the solution of the eigenvalue problem (2.15) determines the sloshing frequencies and their mode shapes for an axisymmetric tank.

### 2.3. Reducing to the system of one-dimensional equations

In formulas (2.10) the surfaces $S$ and $\sigma$ may be either different or coincident ones. If the surface $S$ is the same as $\sigma$ then integrals in Eq.(2.10) are singular and thus the numerical treatment of these integrals has to take into account the presence of this integrable singularity. Integrands here are distributed strongly non-uniformly over the element and standard integration quadratures fail in accuracy.

As in [21, 22] we replace the Cartesian co-ordinates ($x$, $y$, $z$) with cylindrical co-ordinates ($r$, $\theta$, $z$), and take into account that

$$|P - P_0| = \sqrt{r^2 + r_0^2 + (z - z_0)^2 - 2rr_0\cos(\theta - \theta_0)}$$

where points $P$ and $P_0$ have the following coordinates

$$P = (r, z, \theta);\quad P_0 = (r_0, z_0, \theta_0).$$

Representing unknown functions as Fourier series expansions by the circumferential coordinate one can obtain

$$\phi(r, z, \theta) = \phi(r, z)\cos\alpha\theta \qquad (2.16)$$

where $\alpha$ is a given integer (the number of nodal diameters).

After integration in Eq.(2.10) with respect to $\theta$, Eq.(2.16) allows receiving the integral operators Eq,(2.10) as follows

$$\iint_S \phi(P)\frac{\partial}{\partial n}\frac{1}{|P-P_0|}dS = \int_\Gamma \phi(r,z)\Theta(P,P_0)d\Gamma;$$

$$\iint_S \phi(P)\frac{1}{|P-P_0|}dS = \int_\Gamma \phi(r,z)\Phi(P,P_0)d\Gamma; \quad P_0 \in \sigma. \tag{2.17}$$

Here, $\Gamma$ is the generating boundary contour of the surface *S*. Along this contour we have $r = r(z)$; kernels $\Theta(P,P_0)$ and $\Phi(P,P_0)$ are defined as in [20, 21]

$$\Theta(z,z_0) = \frac{4}{\sqrt{a+b}}\left\{\frac{1}{2r}\left[\frac{r^2 - r_0^2 + (z_0-z)^2}{a-b}\mathsf{E}_\alpha(k) - \mathsf{F}_\alpha(k)\right]n_r + \frac{z_0-z}{a-b}\mathsf{E}_\alpha(k)n_z\right\};$$

$$\Phi(P,P_0) = \frac{4}{\sqrt{a+b}}\mathsf{F}_\alpha(k).$$

The following notations are introduced hereinabove

$$\mathsf{E}_\alpha(k) = (-1)^\alpha\left(1-4\alpha^2\right)\int_0^{\pi/2}\cos 2\alpha\theta\sqrt{1-k^2\sin^2\theta}\,d\theta, \qquad \mathsf{F}_\alpha(k) = (-1)^\alpha\int_0^{\pi/2}\frac{\cos 2\alpha\theta d\theta}{\sqrt{1-k^2\sin^2\theta}},$$

$$a = r^2 + r_0^2 + (z-z_0)^2, \quad b = 2rr_0; \qquad k^2 = \frac{2b}{a+b}.$$

Numerical evaluation of integrals in Eqs (2.17) has been accomplished by the BEM with a constant approximation of unknown functions inside elements. It would be noted that internal integrals here are complete elliptic ones of first and second kinds. As the first kind elliptic integrals are non-singular, one can successfully use standard Gaussian quadratures for their numerical evaluation. For elliptic integrals of second kind we have applied here the approach based on the following characteristic property of the arithmetic geometric mean AGM (*a*, *b*) (see [17])

$$\int_0^{\pi/2}\frac{d\theta}{\sqrt{a^2\cos^2\theta + b^2\sin^2\theta}} = \frac{\pi}{2AGM(a,b)}.$$

To define AGM(*a*, *b*) there exists a simple Gaussian algorithm, described below

$$a_0 = a; \quad b_0 = b; \; a_1 = \frac{a_0+b_0}{2}; \quad b_1 = \sqrt{a_0 b_0}; \ldots a_{n+1} = \frac{a_n+b_n}{2}; \quad b_{n+1} = \sqrt{a_n b_n}; \ldots$$

$$\mathrm{AGM}(a,b) = \lim_{n\to\infty} a_n = \lim_{n\to\infty} b_n.$$

It is a very successful method to evaluate the elliptic integrals of the second kind and the effective numerical procedure for inner integrals evaluation, but external integrals in Eq.(2.17) have logarithmic

singularities. So these integrals were treated numerically by special Gauss quadratures applying the technique described in [17].

## 3. Results and discussion

### 3.1. Numerical analysis of low frequency sloshing in cylindrical shells with baffles

The circular cylindrical shell with a flat bottom is considered. Its parameters are as follows: the radius is $R = 1\ m$, the fluid filling level is $H=1.0m$.

Two types of baffles are investigated in this study. First, the baffle is considered as a circle flat plate with a central hole (the ring baffle), (Fig.3a)). The second type of baffle is the conical shell installed into the fluid-filled cylindrical shell, (Figs 3b, 3c)).

The vertical coordinate of the baffle position is $H_1$, the interface surface position is $H_i$, the filling level is $H = H_1 + H_2$ and the radius of the interface surface is $R_i$ (Fig.3d)).

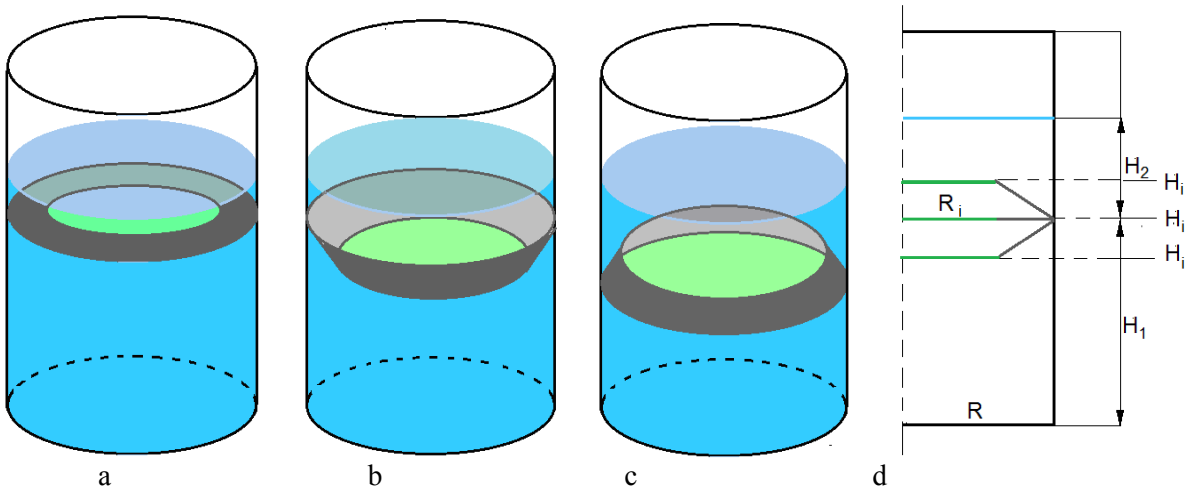


Fig.3. Cylindrical shells with flat (a) and conical (b, c) baffles and their sketch (d).

The main aim of this study is to evaluate the low sloshing frequencies for both axisymmetric and non- axisymmetric vibration modes of baffled cylindrical shells. The numerical solution has been obtained by using the boundary element method (BEM) as it was described beforehand. In the present numerical simulation we used 120 boundary elements along the bottom, 150 elements along wetted cylindrical parts and 120 elements along the radius of free surface. At the interface and baffle surfaces the different numbers of elements depending on the radius of the interface surface were used. Here we study the modes and frequencies of baffled tank in dependence of parameters, $R_i$, $H_i$, $H_1$, namely a radius of the baffle orifice, the free surface position and the vertical coordinate of the baffle position.

The benchmark testing for the partially filled rigid cylindrical shell described above has been performed. The numerical values of the frequency parameter $\chi^2_{\alpha n}/g, \alpha = 0,1; n = \overline{1,5}$ for different numbers of nodal diameters $\alpha$ are compared with analytical solutions of Ibrahim [23] and presented in Tab.1.

In all tables we have compared the eigenvalues (frequency parameter) for the problem described beforehand.

Table 1. Comparison of numerical and analytical values of the frequency parameters.

| $\alpha$ | Method | *n=1* | *n=2* | *n=3* | *n=4* | *n=5* |
|---|---|---|---|---|---|---|
| 0 | BEM | *3.830* | *7.017* | *10.176* | *13.329* | *16.479* |
| | [23] | *3.828* | *7.016* | *10.173* | *13.324* | *16.471* |
| 1 | BEM | *1.750* | *5.332* | *8.538* | *11.709* | *14.870* |
| | [23] | *1.750* | *5.331* | *8.536* | *11.706* | *14.864* |

These results have demonstrated the good agreement and testified the validity of the proposed multi-domain approach.

Tables 2 and 3 hereinafter provide the numerical values of the frequency parameter $\chi^2_{\alpha n}/g$ of liquid sloshing for $\alpha = 0$, $n = \overline{1.5}$ at $H_1=0.5m$ for tanks with flat and conical baffles for $R_i=0.7m$ and $R_i=0.3m$, respectively.

In Tabs 2-3 hereinafter the values $H_1=H_i=0.5m$ correspond to the flat baffle (Fig.3a)), the values $H_1=0.5m$, $H_i=0.4m$ correspond to the conical baffle (Fig.3b)) and the values $H_1=0.5m$, $H_i=0.6m$ correspond to the conical baffle (Fig.3c)). The configuration of baffles shown in Fig.3c) at $R_i=0.3m$ provides a greater reduction of the frequencies.

Table 2. Frequency parameter for tanks with flat and conical baffles, $R_i=0.7m$.

| $H_i$, *m* | *n=1* | *n=2* | *n=3* | *n=4* | *n=5* |
|---|---|---|---|---|---|
| *0.5* | *3.7553* | *7.0124* | *10.1762* | *13.3290* | *16.4791* |
| *0.4* | *3.8186* | *7.0141* | *10.1760* | *13.3289* | *16.4791* |
| *0.6* | *3.7345* | *7.0061* | *10.1761* | *13.3290* | *16.4791* |

Table 3. Frequency parameter for tanks with flat and conical baffles, $R_i=0.3m$.

| $H_i$, *m* | *n=1* | *n=2* | *n=3* | *n=4* | *n=5* |
|---|---|---|---|---|---|
| *0.5* | *3.6698* | *7.0056* | *10.1759* | *13.3290* | *16.4791* |
| *0.4* | *3.7281* | *7.0117* | *10.1762* | *13.3290* | *16.4791* |
| *0.6* | *3.5663* | *6.9878* | *10.1746* | *13.3289* | *16.4791* |

For non- axisymmetric modes ($\alpha = 1$) the numerical values of the frequency parameter $\chi^2_{\alpha n}/g$ $\alpha = 1; n = \overline{1.5}$ with $R_i=0.3m$ for tanks with flat and conical baffles at $H_1=0.5m$ and $H_1=0.8m$ were calculated.

In Tab.4 there are numerical values of the frequency parameter $\chi^2_{\alpha n}/g$ of liquid sloshing for $\alpha = 1; n = \overline{1.5}$ ; $R_i=0.3m$ for tanks with flat and conical baffles at $H_1=0.5m$ and with different $H_i$.

Table 4. Frequency parameter for tanks with flat and conical baffles, $H_1=0.5m$.

| $H_i$, *m* | *n=1* | *n=2* | *n=3* | *n=4* | *n=5* |
|---|---|---|---|---|---|
| *0.5* | *1.3663* | *5.2941* | *8.5359* | *11.7097* | *14.8701* |
| *0.4* | *1.4439* | *5.3087* | *8.5371* | *11.7098* | *14.8701* |
| *0.6* | *1.2714* | *5.2669* | *8.5325* | *11.7092* | *14.8700* |

Table 5 provides the frequency parameter $\chi^2_{\alpha n}/g$ of liquid sloshing for $\alpha = 1; n = \overline{1.5}$ , $R_i=0.3m$ and different values of $H_i$ and $H_1$. The values $H_1=H_i=0.8m$ correspond to the flat baffle (Fig.3a).

Table 5. Frequency parameter for tanks with flat and conical baffles.

| $H_1$, m | $H_i$, m | n=1 | n=2 | n=3 | n=4 | n=5 |
|---|---|---|---|---|---|---|
| 0.8 | 0.8 | 0.7079 | 4.5066 | 8.1947 | 11.5556 | 14.814 |
| 0.8 | 0.7 | 0.8613 | 4.8095 | 8.3640 | 11.6517 | 14.852 |
| 0.8 | 0.9 | 0.5295 | 3.9653 | 7.7559 | 11.1126 | 14.532 |
| 0.9 | 0.8 | 0.5685 | 3.9031 | 7.6628 | 11.1591 | 14.554 |
| 0.7 | 0.8 | 0.8263 | 4.8264 | 8.3813 | 11.6464 | 14.851 |

The three first modes of liquid vibrations (numbers 1, 2, 3) for $\alpha=1$ are shown on Fig.4. Here we consider both un-baffled and baffled tanks. The radius of orifice is here $R_i=0.3m$.

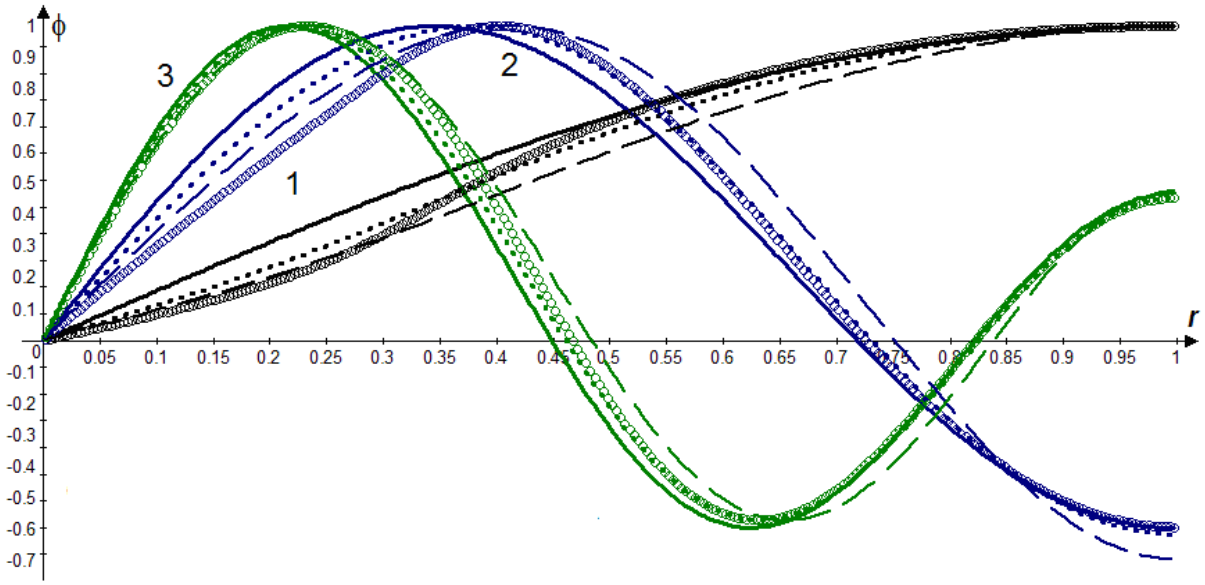


Fig.4. Modes of vibrations of un-baffled and baffled tanks, $\alpha=1$.
_____ - shell without baffle,
..... - shell with flat baffle,
o o o o o - shell with conical baffle at $H_i=0.8m$; $H_1=0.9m$,
__ __ __ - shell with conical baffle at $H_i=0.9m$; $H_1=0.8m$.

The modes of liquid vibrations of baffled and un-baffled tanks are similar, the most essential difference occurs in results for an un-baffled tank and for a tank with conical baffle at $H_i > H_1$.

Installation of any kind of baffles in considered cases provides decreasing of frequencies. This decrease is essential for only first three frequencies both for axisymmetrical ($\alpha=0$) and non-axisymmetrical ($\alpha=1$) modes.

The conical baffles provide a more essential decreasing of frequencies than flat ones.
The baffle configuration corresponded to $H_i=0.9m$; $H_1=0.8m$ and $H_i=0.8m$; $H_1=0.9m$ provides the largest decline in the first three frequencies both for $\alpha=0$, $\alpha=1$.

Figure 5 demonstrates the first sloshing modes both for $\alpha=0$ and $\alpha=1$ for tanks without baffles and with the conical baffle (Fig.3c). Here $H_i=0.6m$; $H_1=0.5m$; $R_i=0.7m$. Figures 5a and 5c demonstrate first modes of liquid vibrations in the cylindrical tank without baffles, for $\alpha=0$ and $\alpha=1$, respectively. Figures 5b and 5d correspond to first modes of liquid vibrations in the cylindrical tank with conical baffles, for $\alpha=0$ and $\alpha=1$, respectively.

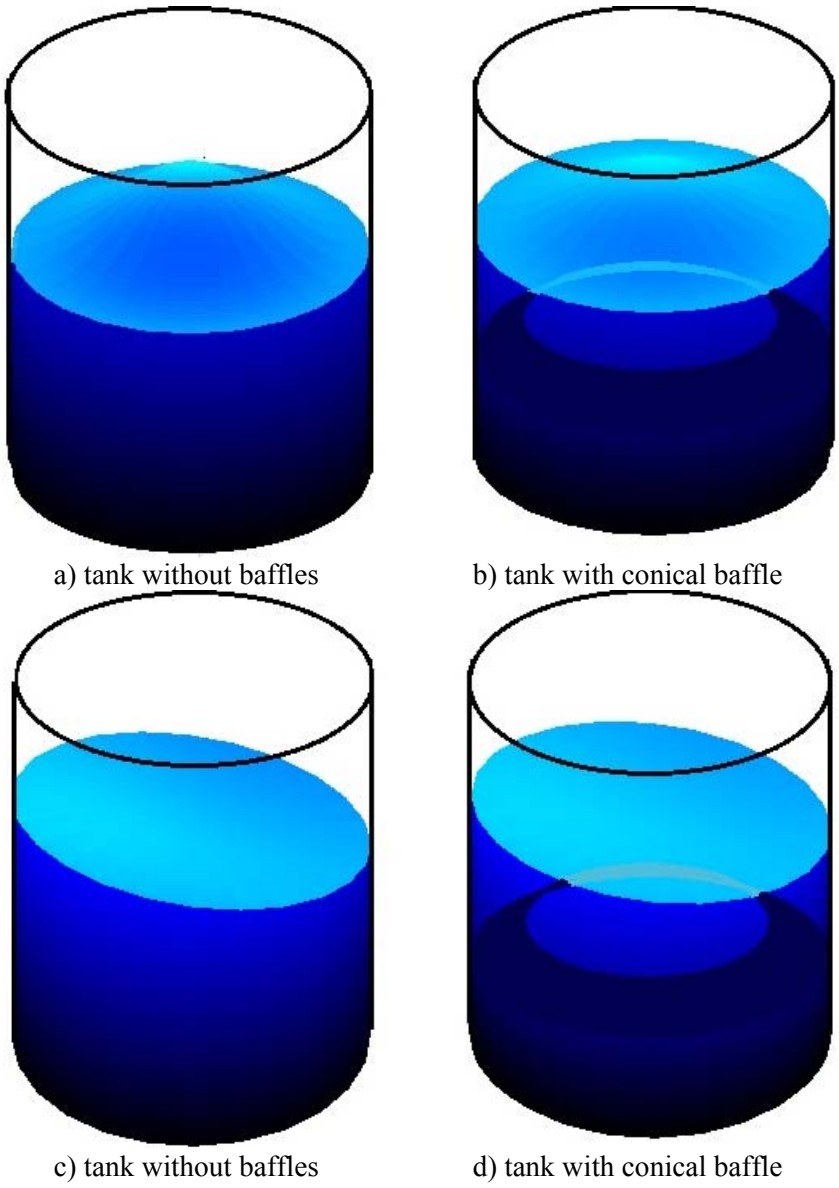

a) tank without baffles b) tank with conical baffle

c) tank without baffles d) tank with conical baffle

Fig.5. Sloshing modes in cylindrical tank without baffles and with conical baffle.

These results demonstrate that modes of vibrations of baffled and un-baffled tanks at $\alpha=1$ differ more significantly when conical baffles are installed.

### 3.2. Areas of further research

This developed approach will be easly generalized for elastic tanks with elastic baffles. The geometry of tank also can be easy changed, so the results will be obtained for conical, spherical and compound shells with and without baffles. The problem statement has provided the possibility of simulating forced vibration. It has to be noted also that the present study is based on the potential flow theory without the inclusion of fluid viscosity and energy dissipations. The effect of factors such as the fluid viscosity on the resonant sloshing in tanks and reservoirs is worthy to be further investigated.

## 4. Conclusions

Sloshing in the tank may be controlled by installing baffles, and the effectiveness highly depends on the shape, the location, and the number of baffles inside a tank. But in practice, the effect of baffles usually can be seen after the baffle has already been installed. Also, the visual inspection of the sloshing event inside the tank is not adequate for baffles design validation. Due to the complexities associated with the sloshing phenomenon, the numerical simulation is an effective method to meet the design intent, and shorten the development time.

The proposed method makes it possible to determine a suitable place with a proper height for installation of the baffles in tanks by using the numerical simulation. The liquid sloshing in the baffled and un-baffled rigid tanks under the force of gravity has been studied. The proposed approach allows us to carry out the numerical simulation of tanks with baffles in the form of a circular flat plate with an orifice and conical baffles of different sizes and with different position in the tank. This gives the possibility of governing both the baffle configuration and its position within the tank. The considered problem was solved using the multi-domain boundary element methods.

## Acknowledgment

The authors thank our collaborators on STCU Project #6247, Professors Carlos Brebbia, Wessex Institute of Technology, UK, and Alexander Cheng, University of Mississippi, USA, for their constant support and interest in our research.

## Nomenclature

$g$ – acceleration due to gravity
$H$ – fluid filling level
$H_1$ – vertical coordinate of the baffle position
$H_i$ – interface surface position
$\boldsymbol{n}$ – external unit normal to the wetted surface
$R$ – radius of circular cylindrical shell
$(r, \theta, z)$ – cylindrical co-ordinates
$q$ – flux
$S_0$ – liquid free surface
$S_w$ – the wall surface,
$S_{\text{baf}}$ – the surface of baffles
$S_{\text{bot}}$ – bottom surface
$t$ – time
$(x, y, z)$ – Cartesian co-ordinates
$\Phi$ – fluid velocity potential

## References

[1] *Space Exploration Technologies Corp. Demo Flight 2* (2007): Flight Review Update, June 15.

[2] Vreeburg, Jan P.B. (2005): *Spacecraft Maneuvers and Slosh Control*.– IEEE Control Systems Magazine.

[3] Strandberg L.(1978): *Lateral Stability of Road Tankers*.– Sweden, VTI Report No. 138A.

[4] Lloyd N., Vaiciurgis E.T.A. and Langrish G. (2002): *The effect of baffle design on longitudinal liquid movement in road tankers: an experimental investigation*. – Process Safety and Environ Prot Trans Inst. Chem. Engrs., vol.80, No.4, pp.181-185.

[5] Wang J.D., Lo S.H. and Zhou D. (2013): *Liquid sloshing in rigid cylindrical container with multiple rigid annular*

*baffles: Lateral vibration*.– Journal of Fluids and Structures, vol.42, pp.421-436.

[6] Younes M.F., Younes Y.K., El-Madah M., Ibrahim I.M. and El-Dannanh E.H. (2007): *An experimental investigation of hydrodynamic damping due vertical baffle arrangements in rectangular tank*. – Proc. I Mech E, J. Eng. Maritime Environ., vol.221, pp.115-123.

[7] Ravnik J., Strelnikova E., Gnitko V., Degtyarev K. and Ogorodnyk U. (2016): *BEM and FEM analysis of fluid-structure interaction in a double tank* .– Engineering Analysis with Boundary Elements, vol.67, pp.13-25.

[8] Gnitko V., Naumenko V., Rozova L. and Strelnikova E. (2016): *Multi-domain boundary element method for liquid sloshing analysis of tanks with baffles*.– Journal of Basic and Applied Research International, vol.17, No.1, pp.75-87.

[9] Popov G., Sankar S. and Sankar T.S. (1993): *Dynamics of liquid sloshing in baffled and compartmented road containers*. – J. Fluids Struct., vol.7, pp.803-821.

[10] Wu C. and Chen B. (2009): *Sloshing waves and resonance modes of fluid in a 3D tank by a time-independent finite difference method*. – Ocean Eng., vol.36, pp.500-510.

[11] Kandasamy T., Rakheja S. and A. Ahmed K.W. (2010): *An analysis of baffles designs for limiting fluid slosh in partly filled tank trucks*. – The Open Transportation Journal, vol.4, pp.23-32.

[12] Mi-an Xue, Peng-zhi Lin, Jin-hai Zheng, Yu-xiang Ma, Xiao-li Yuan and Viet-Thanh Nguyen (2013): *Effects of perforated baffle on reducing sloshing in rectangular tank: Experimental and numerical study*. – China Ocean Engineering, vol.27, No.5, pp.615-628.

[13] Eswaran M., Saha U.K. and Maity D. (2009): *Effect of baffles on a partially filled cubic tank: Numerical simulation and experimental validation*. – Journal of computer and structures, vol.87, pp.198-205.

[14] Abbas Maleki and Mansour Ziyaeifar (2008): S*loshing damping in cylindrical liquid storage tanks with baffles*. – Journal of Sound and Vibration, vol.311, No.1–2, pp.372–385.

[15] Jin Yan and Hong Liang Yu (2011): *The free sloshing modal analysis of liquid tank with baffles*. – Advanced Materials Research, vol.10, pp.347-353.

[16] Gavrilyuk I., Lukovsky I., Trotsenko Yu. and Timokha A. (2006): *Sloshing in a vertical circular cylindrical tank with an annular baffle. Part 1. Linear fundamental solutions*. – Journal of Engineering Mathematics, vol.54, pp.71-88.

[17] Degtyarev K., Glushich P., Gnitko V. and Strelnikova E. (2015): *Numerical simulation of free liquid-induced vibrations in elastic shells*. – International Journal of Morern Physics and Applications, vol.1, No.4, pp.159-168.

[18] Liu D. and Lin P. (2008): *A numerical study of three-dimensional liquid sloshing in tanks*. – J. Comput. Phys., vol.227, pp.3921-3939.

[19] Kashani B.K. and Sani A.A. (2016): *Free vibration analysis of horizontal cylindrical shells including sloshing effect utilizing polar finite elements*. – European Journal of Mechanics and Solids, vol.58, pp.187-201.

[20] Brebbia C.A., Telles J.C.F. and Wrobel L.C. (1984): *Boundary Element Techniques.* – Berlin and New York: Springer-Verlag.

[21] Degtyarev K., Gnitko V., Naumenko V. and Strelnikova E. (2016): *Reduced boundary element method for liquid sloshing analysis of cylindrical and conical tanks with baffles*. – Int. Journal of Electronic Engineering and Computer Sciences, vol.1, pp.14-27.

[22] Ventsel E., Naumenko V., Strelnikova E. and Yeseleva E. (2010): *Free vibrations of shells of revolution filled with a fluid.* – Engineering Analysis with Boundary Elements, vol.34, pp.856-862.

[23] Ibrahim R.A. (2005): *Liquid Sloshing Dynamics: Theory and Applications*. – Cambridge University Press.

Received: April 17, 2017

Revised: June 16, 2017